Dynamic Primitives and Optimal Feedback Control for the Manipulation of Complex Objects

Reza Sharif Razavian*, Salah Bazzi, Rashida Nayeem, Mohsen Sadeghi, and Dagmar Sternad

Abstract— **Modern computer algorithms easily beat world champions in chess or Go, but state-of-the-art robots are still outperformed by two-year-old's in manipulating the pieces, let alone interacting with more complex objects. This work studied human behavior when moving an underactuated object, a cup with a ball rolling inside creating internal dynamics like sloshing coffee in a cup. The objective was to develop a control model that could replicate human behavior. Human movement data were collected for transporting this cup-and-ball system, both with and without external perturbations. The existing models in the human control literature, including maximum smoothness, optimal feedback control with minimum effort, and dynamic primitives with impedance were revisited for this challenging task. As these control models were primarily developed for unconstrained reaching movements, they could replicate human trajectories when transporting a rigid object. However, they fell short when the object introduced complex interaction forces due to its internal dynamics. Therefore, this study extended the framework of dynamic primitives and used an optimal controller to generate a maximally smooth zero-force trajectory for the impedance operator when interacting with perturbations from the object or the environment. Given the challenges that robot control still faces when interacting with complex objects, these findings may inform the development of bio-inspired controllers for robotic manipulation.**

I. INTRODUCTION

Despite significant advances in robot design and control, human-like agility and dexterity has yet to be achieved in robots, and much remains to be learned from human movement control. Human and animal behavior has inspired the development of many novel ideas and concepts in robotics; for example, adaptive impedance-based control of manipulators for physical interactions [1], central pattern generators [2], exploitation of passive dynamics in locomotion [3], [4], and many elements in the design and control of soft robots [5], [6].

While state-of-the-art robotic manipulators are adept at picking and placing rigid objects [7], they still struggle in manipulating more complex objects such as flexible materials, articulated objects, and containers with liquids. Most of the approaches to the interaction with complex objects rely on developing more accurate models and simulations [8], however modeling every possible object a robot might encounter is not practical. Recent work has progressed towards robot control without relying on high-fidelity models, e.g., manipulating deformable objects [9]. However, this approach assumes that the robot is quasi-static which makes this control strategy not applicable to situations where dynamic motion is involved. To gain further insight and potentially inform and advance control algorithms, this study examines how humans control objects with complex internal dynamics.

To date, studies on human motor control have predominantly focused on reaching and pointing tasks, devoid of any contact or interaction with dynamic objects. Only very few studies have gone beyond rigid objects and investigated the control of a linear mass-spring system [10]–[12], a cart-and-pendulum system [13] and a whip [14], [15]. These studies revealed that the principles that are sufficient for simple human movements do not generalize to more complex physical interactions. Instead, objectives such as predictability [16], stability of the underactuated object [17], [18], or minimization of transient duration [19] have come to the fore. For the task of bringing a dynamic object to rest humans exploit the internal dynamics of the object [11], [12], [20]. These novel computational analyses have shed light on the richness of the human capabilities. However, a generative model that can synthesize the human behavior in such complex tasks is yet to be developed.

In computational movement neuroscience, several control models have been proposed and validated for the task of goal-directed reaching in the horizontal plane. One of the earliest control models has been inspired by the straightness of hand trajectories in kinematic space associated with a bell-shaped velocity profile [21]. It was then shown that these features are replicated when the third derivative (jerk) of the hand trajectory is minimized (i.e., smoothness is optimized) [22], [23].

A conceptually distinct model that has successfully replicated key features of human behavior in these reaching tasks is stochastic optimal feedback control (OFC), specifically when it trades off minimum effort for kinematic accuracy [24], [25]. This OFC model could account for human movements and adaptations to state-dependent force fields [26], perturbations [27], and distortions in visuo-motor mappings [28]. The minimum-variance model [29] that could replicate the speed-accuracy trade-off, observed in numerous human behaviors, has been shown to be equivalent to OFC when minimizing effort [30].

One other distinct approach are dynamic primitives that has been developed in both human studies and robotics [31]–[34]. Instead of relying on pre-planned trajectories, human or robot movement trajectories are generated via building blocks that have stability, i.e., dynamic attractors. Two basic

*Corresponding author: r.sharifrazavian@northeastern.edu. All authors are in the Departments of Biology, Electrical and Computer Engineering,and Physics, Northeastern University, Boston, MA, USA. The research was funded by NSERC Postdoctoral Fellowship (Reza Sharif Razavian) and NSF-NRI-1637854, NSF-M3X-1825942 and NIH-R01-HD087089, awarded to Dagmar Sternad. Authors also thank Mr. Piet Lammertse for continued technical assistance.

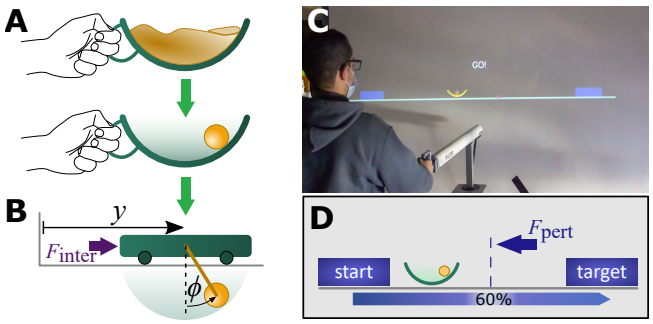

Fig. 1: The cup-and-ball experimental paradigm. **A**. The liquid inside the cup is approximated by a ball rolling inside a circular cup. **B**. The cup-and-ball model is equivalent to a cart-and-pendulum system. **C.** The cup-and-ball system simulated in the virtual environment; participants interact with it by moving a haptic robot. **D**. The task is to move the cup to the target without losing the ball.

primitives are discrete and rhythmic attractors that are parameterized and combined to create more complex behaviors. In robotics, dynamic movement primitives (DMPs) have been used to teach robots how to perform a variety of behaviors from human demonstrations, such as tennis swings [35], grasping [36], and playing drums [37]. However, DMPs are constrained to learning from explicit demonstration. In human neuroscience, Sternad and colleagues proposed dynamic models for these two basic attractors and demonstrated how their combination can reproduce a variety of unimanual and bimanual behaviors [31], [38], [39]. More recently, Hogan and Sternad extended the set of fundamental dynamic primitives by including mechanical impedance to specifically address physical interactions with objects [40]. Thus, in the context of interacting with an object or the environment, the primitives are used to determine the 'zero-force trajectory' of the impedance operator. However, it is yet to be determined how this zero-force trajectory is generated for the interaction with a complex object.

While these models have all been successful in capturing important features of human movements in tightly constrained experimental tasks, their ability generalize to more complex behaviors, such as manipulation of underactuated systems, has not yet received attention. Hence, the first aim of this work was to evaluate extant control models in their ability to replicate human behavior for the control of a complex underactuated object. The second aim used these insights and developed a unifying control framework that could replicate human behavior in both simple and complex interactions. This work may inform the development of control algorithms for dexterous robotic manipulation.

II. Methods

A. Complex Object: A Ball in a Cup

In order to gain further insight into human motor control, a rich test bed with dynamically complex control challenges is needed. Our work has taken inspiration from the daily activity of carrying a cup of coffee; the dynamics of the coffee creates nonlinear interaction forces acting on the hand [16], [18]. Such nonlinear and potentially chaotic interaction forces require control mechanisms that are absent in unconstrained reaching, even when exposed to the linear state-dependent force fields commonly studied in the human control literature. To make the complex task scientifically repeatable and computations tractable, the dynamic effects of the sloshing liquid inside the cup were simplified to a sliding ball inside a 2-D cup (Fig. 1A). This cup-and-ball system is equivalent to a 2-D cart-and-pendulum system (Fig. 1B) with the equations of motion:

$$(M+m)\ddot{y} = ml\left(\dot{\phi}^2\sin(\phi) - \ddot{\phi}\cos(\phi)\right) + F_{inter} + F_{pert}, \quad (1)$$

$$l\ddot{\phi} = -g\sin(\phi) - G\ddot{y}\cos\phi, \quad (2)$$

where y and ϕ are the cup position and ball angle, respectively. F_{inter} is the force of the hand interacting with the cup, and F_{pert} is a perturbation force. System parameters $M = 3$ kg and $m = 0.3$ kg are the cup and ball masses, respectively. The pendulum length $l = 0.5$ was also the radius of the cup, $g = 9.81$ m/s^2 is the gravitational acceleration, and $G = 5$ is the coupling term between the cup and the ball dynamics. To make the control synthesis easier, the cup-and-ball system was linearized around zero-states. The same linearized equations are simulated in the virtual environment:

$$(M+m)\ddot{y} = -ml\ddot{\phi} + F_{inter} + F_{pert}, \quad (3)$$

$$l\ddot{\phi} = -g\phi - G\ddot{y}. \quad (4)$$

B. Experimental Procedure

Four participants (3 men, 21-33 yrs) took part in this study. They gave written informed consent as approved by the Institutional Review Board at Northeastern University. The cup-and-ball system was simulated in a virtual environment, and participants interacted with the simulated system via a haptic robotic interface that provided force feedback according to the dynamics of the cup and ball (Fig. 1C). Participants were instructed to move the cup at their self-selected speed via moving the robot's handle along a horizontal line to arrive at a target box 40 cm to the right of their start point (Fig. 1D). Participants were instructed that the ball should not 'escape' from the cup, i.e., its angle should not exceed the cup's rim ($\phi_{rim} = \pm 45°$). Each participant performed 3 sessions of 100 trials each with the following 3 conditions: In condition 1, the ball was rigidly attached to the bottom of the cup, forming a single rigid object; in condition 2, the ball could freely roll inside the cup making the system underactuated; in condition 3, an impulse-like perturbation was applied to the system in opposite direction of the cup movement at 60% of the travel distance. This perturbation was applied in all 100 trials. The order of the three conditions was identical for all participants.

In the virtual environment, the system was initialized with $y_0 = -0.4$, $\dot{y}_0 = 0, \phi_0 = 0, \dot{\phi}_0 = 0$, and the target box was located at $y_f = 0$. In the rigid-object condition, the ball dynamics was removed and only an inertia $(M+m)$ was simulated in the virtual environment. In the perturbation trials, $F_{pert} = -20$ N and lasted for 20 ms when the cup first reached 60% of the travel distance, and was zero otherwise.

C. Existing Motor Control Models

Although models in the human control literature are less granular than those in robotics, many of their core ideas are comparable to those in robotics: (1) Planning of actions in kinematic space as maximally smooth trajectories (minimum-jerk model, Fig. 2A), (2) Execution of actions via optimally tuned feedback gains (optimal feedback control model, Fig. 2B), and (3) Formation of actions as an evolution of a dynamical system following attractor dynamics (dynamic primitives model, Fig. 2C). Each of these concepts will be tested against experimental data, and their merits will be assessed in the context of the cup-and-ball task. Then the strengths of these models can be combined and tailored into a new framework.

1) Maximum Smoothness in Kinematic Space: Unconstrained point-to-point reaching movements tend to have straight linear paths in kinematic space with bell-shaped velocity profiles that exhibit high smoothness [22]. This robust observation supported that humans favor smoothness in kinematic space in goal-oriented tasks. The maximally smooth hand (cup) trajectory is mathematically defined as the one that minimizes jerk, i.e, time-derivative of acceleration, during the movement:

$$y^*(t) = \arg\min \left\{ \int_0^{t_f} \left(\frac{d^3 y(t)}{dt^3} \right)^2 dt \right\}, \tag{5}$$

given the boundary conditions:

$$y(0) = y_0, \quad y(t_f) = y_f, \tag{6}$$

$$\dot{y}(0) = \ddot{y}(0) = \dot{y}(t_f) = \ddot{y}(t_f) = 0, \tag{7}$$

which results in a fifth-order polynomial trajectory:

$$y^*(t) = \tag{8}$$
$$y_0 + (y_f - y_0) \left(10 \left(\tfrac{t}{t_f} \right)^3 - 15 \left(\tfrac{t}{t_f} \right)^4 + 6 \left(\tfrac{t}{t_f} \right)^5 \right).$$

This control principle implies that humans bring their hand from a given start position to stop at the target in a given time via a pre-determined trajectory. This feed-forward hand trajectory can be used to drive the cup-and-ball system (Fig. 2D). It must be noted that this model accounts for hand motion in free space, but does not specify hand movement in an interactive context, nor can it predict how the behavior may change in response to perturbations. Therefore, this model alone is insufficient to explain complex interactions.

2) Optimal Feedback Control: A different model applied to human movement control postulates that humans control their movements by optimizing certain objectives such as minimal effort [24]. Behavioral observations such as smoothness and compliance in physical interactions result from optimally adjusted feedback gains [41] obviating the need for a pre-planned trajectory (Fig. 2B). In this optimal feedback control (OFC) framework, human control is approximated by a linear quadratic Gaussian (LQG) controller that includes the noise characteristics of the neuromuscular system [25]. The optimal controller minimizes the quadratic cost function:

$$J = \sum_{t=0}^{N-1} \left(\mathbf{x}_t^T \mathbf{Q}_t \mathbf{x}_t + \mathbf{u}_t^T \mathbf{R}_t \mathbf{u}_t \right) + \mathbf{x}_N^T \mathbf{Q}_N \mathbf{x}_N, \tag{9}$$

subject to the constraint:

$$\mathbf{x}_{t+1} = \mathbf{A}_t \mathbf{x}_t + \mathbf{B}_t \left(\mathbf{I} + \boldsymbol{\varepsilon}_t \right) \mathbf{u}_t + \boldsymbol{\xi}_t, \tag{10}$$

where $\mathbf{x} \in \mathbb{R}^n$ is the state vector, and $\boldsymbol{\xi}$ and $\boldsymbol{\varepsilon}\mathbf{u}$ represent additive and control-dependent noise terms, respectively. It is further assumed that the states can only be estimated from the d-step-delayed sensory information that is affected by additive ($\boldsymbol{\omega}$) and state-dependent ($\boldsymbol{\epsilon}\mathbf{x}$) noise:

$$\mathbf{y}_t = \mathbf{H}_t \left(\mathbf{I} + \boldsymbol{\epsilon}_t \right) \mathbf{x}_{t-d} + \boldsymbol{\omega}_t. \tag{11}$$

The linear state-space model for the cup-and-ball system is:

$$\mathbf{x}_t = \left[y_t,\ \phi_t,\ \dot{y}_t,\ \dot{\phi}_t, F_t \right]^T \tag{12}$$

$$\mathbf{A} = \begin{bmatrix} 0 & 0 & 1 & 0 & 0 \\ 0 & 0 & 0 & 1 & 0 \\ 0 & \frac{mg}{\alpha} & 0 & 0 & 1/\alpha \\ 0 & \frac{-g}{l}(1 + \frac{Gm}{\alpha}) & 0 & 0 & \frac{-G}{l\alpha} \\ 0 & 0 & 0 & 0 & -1/\tau \end{bmatrix} \tag{13}$$

$$\mathbf{B} = [0,\ 0,\ 0,\ 0,\ 1/\tau]^T \tag{14}$$

$$\mathbf{H} = \mathbf{I}_{n \times n} \tag{15}$$

which needs to be time-discretized (Euler integration with time-step δt =10 ms). The fifth state in this state space represents an equivalent muscle force with dynamics approximated by a first-order filter of the scalar neural input u with time constant $\tau = 30$ ms [42]. The shorthand variable is defined as $\alpha = m + M - mG$ for the isolated cup-and-ball system. However, to be consistent with prior models in the human literature, an equivalent arm mass was added to the cup (Fig. 2E), so that the input represents muscular effort rather than interaction force; i.e., $\alpha = m + (M + M_a) - mG$ with $M_a = 4$ kg [26] as the equivalent arm mass.

When modeling human motor actions, OFC often minimizes the control effort (approximating neuromuscular activity) and the kinematic error from the target [25]. Thus, the positive semi-definite matrices in the objective functions (9) are defined as follows for the cup-and-ball system:

$$\mathbf{Q}_t = \text{Diag}\left(\left[0,\ 10^2\ (rad^{-1}),\ 0,\ 0,\ 0 \right] \right),\ \forall t \neq N \tag{16}$$

$$\mathbf{Q}_N = \text{Diag}\left(\left[10^5\ (m^{-1}),\ 0,\ 10^5\ (sm^{-1}),\ 0,\ 0 \right] \right) \tag{17}$$

$$\mathbf{R}_t = 1\ (N^{-1}),\ \forall t \tag{18}$$

One limitation of this OFC formulation is that state constraints to mimic the task instruction of 'not losing the ball' cannot be added explicitly. As a proxy, a small penalty term for the ball angle (second state) was included in (16) to discourage large ball angles during the motion. The result of this OFC model is an optimal control law in the form of feedback gain $u_t^* = \mathbf{L}_t \bar{\mathbf{x}}_t$, which drives the cup-and-ball system to the target. It only uses the full-state feedback that is estimated from the delayed sensory information (Fig. 2E).

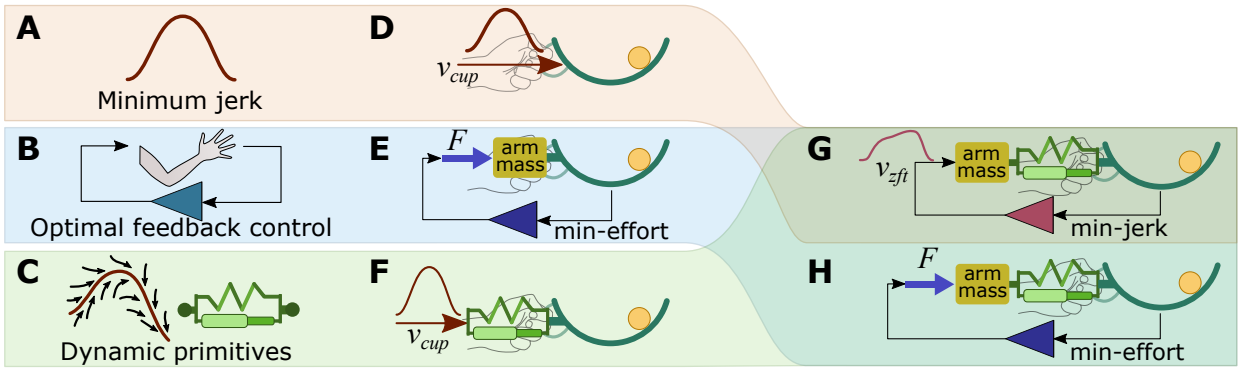

Fig. 2: Core models in human motor control (**A-C**), their implementations for the cup-and-ball system (**D-F**), and two models combining dynamic primitives with optimal feedback control to generate zero-force trajectories (**G,H**). **A.** Movements minimize jerk, or maximize smoothness in kinematic space. **B.** Movements are generated via optimally tuned feedback loops. **C.** Movements evolve as stable trajectories according to attractor dynamics. **D.** The cup is driven with a feed-forward minimum-jerk trajectory. **E.** An optimal feedback controller that minimizes effort. **F.** Cup movements are generated by a feed-forward minimum-jerk trajectory with an impedance primitive. **G.** The zero-force trajectory control model that minimizes jerk. **H.** The zero-force trajectory controller that minimizes effort.

Although the OFC model has successfully captured several characteristics of human reaching [41], it cannot integrate task features inherent to transporting a 'cup-of-coffee' (see Results), necessitating further modifications.

3) Dynamic Primitives for Physical Interactions: Dynamic motion primitives (DMPs) have been used successfully in robotics for trajectory planning and imitation learning [33], [34], [43], [44]. For human motor control, Sternad and colleagues showed that discrete and rhythmic movements and their combinations are well accounted for by discrete fixed-point and limit-cycle attractor dynamics [38], [39]. However, for physical interactions mechanical impedance is needed to augment the attractor dynamics, [45] and was added as a third primitive [40] (Fig. 2C). Importantly, the submovements and oscillators (for discrete and rhythmic movements, respectively) are stable attractors that drive the unrestricted movements. In the case of physical interaction, mechanical impedance is included and discrete and rhythmic components drive the *zero-force trajectories* [46]. In robotics applications, stable trajectory attractors are often constructed using canonical forcing terms [34] independent of the interaction dynamics. In human motor control, proxies for generating the zero-force trajectory have been used, specifically minimum-jerk submovements for discrete movements and sinusoidal oscillations for rhythmic movements [47].

When adding a linear spring-and-damper system with parameters $k_p = 40$ N/m and $k_d = 50$ Ns/m [19] and its zero-force trajectory, y_{zft}, (Fig. 2F), the resulting system dynamics equations are:

$$(M+m)\ddot{y} = -ml\ddot{\phi} + k_p(y_{zft} - y) + k_d(\dot{y}_{zft} - \dot{y}) + F_{pert}, \quad (19)$$

$$l\ddot{\phi} = -g\phi - G\ddot{y}. \quad (20)$$

The dynamic primitives framework has so far remained unspecific about how the zero-force trajectories are generated for more complex interactive tasks. The zero-force trajectory may be represented by the pre-planned minimum-jerk trajectory of (8), or be calculated through other processes. In the present work (Fig. 2F), a minimum-jerk submovement (8) was used as y_{zft} in (19) to drive the system to target in the specified time.

D. Proposed Model: Zero-Force-Trajectory Control

The results revealed several insufficiencies of these existing models. To address these shortcomings, a novel model is proposed to capture the features of the human behavior as measured experimentally. The zero-force trajectory in the dynamic primitives framework needs to be generated in accordance with the dynamics of the object and the requirements of the task—a missing feature in the existing formulation. Optimal feedback control can fill this void by generating a dynamic attractor landscape from optimally tuned feedback gains that produces the zero-force trajectory. Note that in the absence of interactions, the zero-force trajectory and the actual hand path coincide, and the model reduces to the original OFC that produces a smooth minimum-jerk velocity profile.

In tailoring the OFC model to generate zero-force trajectories, we build on the model in (19) that includes mechanical impedance. Instead of assuming a pre-planned zero-force trajectory, y_{zft} is now produced online by the optimal feedback controller. Two features of this approach need to be highlighted: first, the dynamics of the object are taken into account in the formation of the zero-force trajectory; second, the trajectory is generated by a dynamic attractor (via feedback gains) and the trajectory itself changes in response to the evolving system dynamics, including potential perturbation. In this modification there are two choices for the objective function: (1) maximize the smoothness of the zero-force trajectory (Fig. 2G), or (2) minimize the effort generating the zero-force trajectory (Fig. 2H).

1) Zero-Force Trajectory Control with Optimal Effort: The most direct modification is to implement an effort-minimizing optimal feedback controller in the novel framework. OFC sets the optimal forces driving the impedance operator (Fig. 2F). Note that a non-zero mass is needed between the driving force and impedance operator, which is assumed to be the same as M_a for consistency with previous

models. In this effort-minimizing controller, the terms of the cost function are kept the same as (16)-(18), and the state-space equations become:

$$\mathbf{x}_t = \Big[y_t,\ \phi_t,\ \dot{y}_t,\ \dot{\phi}_t, F_t,\ y_{zft},\ \dot{y}_{zft}\Big]^T \tag{21}$$

$$\mathbf{A} = \tag{22}$$

$$\begin{bmatrix} 0 & 0 & 1 & 0 & 0 & 0 & 0 \\ 0 & 0 & 0 & 1 & 0 & 0 & 0 \\ \frac{-k_p}{\alpha} & \frac{mg}{\alpha} & \frac{-k_d}{\alpha} & 0 & 0 & \frac{k_p}{\alpha} & \frac{k_d}{\alpha} \\ \frac{k_pG}{l\alpha} & \frac{-g}{l}(1+\frac{Gm}{\alpha}) & \frac{k_dG}{l\alpha} & 0 & 0 & \frac{-k_pG}{l\alpha} & \frac{-k_dG}{l\alpha} \\ 0 & 0 & 0 & 0 & -1/\tau & 0 & 0 \\ 0 & 0 & 0 & 0 & 0 & 0 & 1 \\ \frac{k_p}{M_h} & 0 & \frac{k_d}{M_h} & 0 & 0 & \frac{-k_p}{M_h} & \frac{-k_d}{M_h} \end{bmatrix}$$

$$\mathbf{B} = [0,\ 0,\ 0,\ 0,\ 1/\tau,\ 0,\ 0]^T \tag{23}$$

$$\mathbf{H} = \mathbf{I}_{n\times n} \tag{24}$$

2) Zero-Force Trajectory Control with Optimal Smoothness: Inspired by the smoothness in kinematic space during unperturbed reaching movements, the OFC model is modified to maximize the smoothness of the zero-force trajectory (minimizing jerk) instead of minimizing the effort. Note that in the absence of physical interaction, this model reduces to the original minimum-jerk model, but without specifying the trajectory *a priori* as a function of time. The objective of maximum smoothness is achieved by substituting the input neural command with the input jerk profile ($u = \frac{d}{dt}(\ddot{y}_{zft})$) and considering $\ddot{y}_{zft}$ as another state:

$$\mathbf{x}_t = \Big[y_t,\ \phi_t,\ \dot{y}_t,\ \dot{\phi}_t, y_{zft},\ \dot{y}_{zft},\ \ddot{y}_{zft}\Big]^T \tag{25}$$

$$\mathbf{A} = \tag{26}$$

$$\begin{bmatrix} 0 & 0 & 1 & 0 & 0 & 0 & 0 \\ 0 & 0 & 0 & 1 & 0 & 0 & 0 \\ \frac{-k_p}{\alpha} & \frac{mg}{\alpha} & \frac{-k_d}{\alpha} & 0 & \frac{k_p}{\alpha M_h} & \frac{k_d}{\alpha M_h} & 0 \\ \frac{k_pG}{l\alpha} & \frac{-g}{l}(1+\frac{Gm}{\alpha}) & \frac{k_dG}{l\alpha} & 0 & \frac{-k_pG}{l\alpha} & \frac{-k_dG}{l\alpha} & 0 \\ 0 & 0 & 0 & 0 & 0 & 1 & 0 \\ 0 & 0 & 0 & 0 & 0 & 0 & 1 \\ 0 & 0 & 0 & 0 & 0 & 0 & 0 \end{bmatrix}$$

$$\mathbf{B} = [0,\ 0,\ 0,\ 0,\ 0,\ 0,\ 1]^T \tag{27}$$

$$\mathbf{H} = \mathbf{I}_{n\times n} \tag{28}$$

The state penalty matrix in the objective function $\mathbf{Q}_t$ in (16) and (17) remains unchanged. However, the control penalty is set to $\mathbf{R}_t = 0.1\ \mathrm{s}^3/m$ to have comparable orders of magnitude of terms in the cost function.

E. Quantification of Models' Goodness-of-Fit

Normalized root-mean-squared (RMS) error between a simulated trajectory and the data was calculated as

$$e_{\aleph} = \mathrm{RMS}(\aleph_{sim} - \aleph_{data})/\mathrm{RMS}(\aleph_{data}) \tag{29}$$

for variables $\aleph \in \{y, \dot{y}, \phi, \dot{\phi}, F_{inter}\}$. A models' prediction error was then defined as the average of $e_{\aleph}$ for all variables. Variability in the data was also quantified using (29) by replacing $\aleph_{sim}$ with mean($\aleph_{data}$), which gave the lower-bound for achievable prediction error.

TABLE I: Models' goodness-of-fit to participants' data

	Rigid	Cup-and-ball	Cup-and-ball perturbed
FF min-jerk	28.2%	51.9%	68.2%
FF min-jerk+imp	33.7%	45.6%	48.1%
OFC min-effort	33.8%	50.6%	53.3%
ZFT min-effort	27.9%	48.1%	47.2%
ZFT min-jerk	26.5%	24.9%	33.0%
Data variability	26.7%	23.8%	28.2%

III. Results

A. Results for Unperturbed Movements

When moving a rigid object, participants exhibited the expected bell-shaped velocity profiles as no additional ball forces acted on the hand (Fig. 3A). Not surprisingly, when manipulating the cup-and-ball system, subjects' trajectories visibly deviated from these smooth profiles (Fig. 3B). After a relatively rapid increase the velocity remained close to constant, followed by a deceleration to stop at the target. Even though participants encountered the same perturbation repeatedly, there was no visible improvement across the 100 trials in any of the conditions.

The smooth bell-shaped velocity profile and interaction forces in the rigid-object condition are well represented by all models (overlaid in Fig. 3A). Further, all models exhibit prediction errors that are close to the the average trial-by-trial differences in participants' data (TABLE. I), rendering them indistinguishable in such simple tasks. Once the ball dynamics is included, the modeled trajectories start to diverge (Fig. 3B, TABLE. I). By design, the feed-forward minimum-jerk model does not adapt to the ball dynamics. When this feed-forward model includes an impedance operator with biologically-plausible values of stiffness and damping, the force from the rolling ball is not large enough to capture the pattern of human movements. However, these small ball forces affect the behavior of the minimum-effort OFC model, and lead to much larger speed modulations than those observed in human behavior. Specifically, as the ball rolls forward and decelerates the cup, the OFC model does not attenuate this deceleration as it minimizes effort. These simulation results resemble those of the OFC where the zero-force trajectory is driven by minimal effort.

In contrast, the zero-force trajectory controller with optimal smoothness penalizes variations in the cup trajectory when encountered with ball forces; consequently, it most closely resembles the experimental profile of cup velocity. Furthermore, due to the underactuated ball dynamics, subtle differences in cup velocity cause large changes in ball angle and interaction forces. This zero-force trajectory controller also reproduces profile features in ball angle and interaction forces, resulting in the lowest prediction error (TABLE. I).

B. Results for Perturbed Cup-and-Ball Movements

Sudden impulse-like perturbations were used to further elicit distinctive characteristics in human behavior to identify

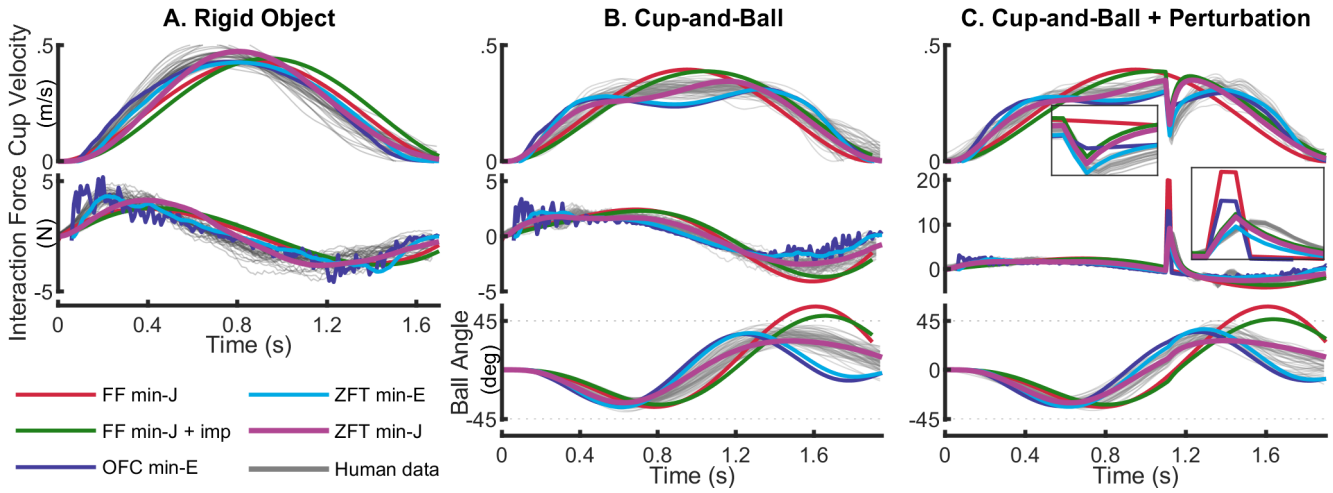

Fig. 3: Human data and simulation results. Gray lines represent one exemplary participants' data, and colored lines are model predictions. Cup velocity, interaction force (between hand and cup), and ball angle are shown. **A**. Rigid object manipulation: All models predict bell-shaped velocity profiles as observed in human data and recreate interaction forces equally well. **B**. Cup-and-ball manipulation: Only the zero-force trajectory controller with optimal smoothness predicts the cup velocity, ball angle, and interaction force profiles that match human behavior. **C**. Cup-and-ball manipulation with external perturbation: Models without hand impedance (effort-minimizing OFC and FF minimum-jerk) do not capture compliant behavior at perturbation and exhibit small velocity change and large spike in interaction force. The zero-force trajectory controller with optimal smoothness fits the human data best.

the controller. When experiencing a resistive perturbation the participant's data in Fig. 3C shows large cup decelerations that are followed by a smooth recovery within approximately 200 ms. Evidently, the models without an impedance do not capture this response to perturbations. The OFC minimum-effort model responds with very 'stiff' behavior to the perturbation, characterized by a small change in velocity, reduced velocity recovery, and large transfer of the perturbation force to the hand (highlighted in the insets in Fig. 3C). The models that include impedance (the two zero-force trajectory controllers and the feed-forward minimum-jerk model with impedance) show compliant responses that are closer to human behavior. This result suggests that feedback gains alone cannot account for arm stiffness, as suggested before [48]. Similar to the unperturbed condition, the dynamics-informed zero-force trajectory controller with optimal smoothness matches the human data most closely.

IV. Discussion

This study investigated human motor control of a complex underactuated object to reveal control priorities that may inform the development of more dexterous robots. Human experiments on a task inspired by 'transporting a cup of coffee' rendered kinematic data that were used as basis to test a range of extant and novel control models. Previous studies of the same cup-and-ball system showed that humans prioritized alternative objectives, such as dynamic stability [18], [49] and predictability and safety margins [13], [16], [19], [50]. To utilize such insights in robot control design, it is necessary to isolate the key features of the human movement controller in a generative model that can reproduce human-like behavior in dynamically complex tasks. Our results showed that when moving a rigid object, the human trajectories displayed smooth bell-shaped velocity profiles that were accounted for by all models. However, the interaction with the cup-and-ball system resulted in forces that acted on the hand and needed to be compensated. These perturbed profiles presented noticeably greater challenges for the models, not only for the feed-forward models, but also for optimal feedback control that minimized effort. When exposed to additional external perturbations, the candidate models differentiated themselves even further.

The model that best replicated human behavior was the zero-force trajectory controller with optimal smoothness that integrated three concepts. The first was the physical interaction via mechanical impedance, which has been shown critical for the stability of human object manipulation [51], [52]. The second concept was an optimal feedback controller that was used to form stable zero-force trajectories, which drove the system toward the target without requiring a pre-planned trajectory. The third concept, minimizing jerk, was the objective in the optimal controller.

The relevance of mechanical impedance to the optimal control framework has been demonstrated before in an open-loop context in musculo-skeletal simulations [53], [54]. Furthermore, Dingwell and colleagues proposed a dynamically-constrained minimum-jerk model for the manipulation of a linear underactuated object [10] which, unlike the zero-force trajectory controller, was formulated as a feed-forward trajectory planning. Lastly, the notion of creating a dynamic attractor for trajectory planning is widely explored in imitation learning [55]. However, the proposed zero-force trajectory controller creates these attractors autonomously via optimally tuned gains instead of human demonstration. The proposed model is an important first step towards identifying the architecture of the human controller and capturing human dexterity in a mathematical form.

REFERENCES

[1] G. Ganesh, A. Albu-Schäffer, M. Haruno, M. Kawato, and E. Burdet, "Biomimetic motor behavior for simultaneous adaptation of force, impedance and trajectory in interaction tasks," *Proceedings - IEEE International Conference on Robotics and Automation*, pp. 2705–2711, 2010.

[2] A. J. Ijspeert, A. Crespi, D. Ryczko, and J.-M. Cabelguen, "From swimming to walking with a salamander robot driven by a spinal cord model." *Science (New York, N.Y.)*, vol. 315, no. 5817, pp. 1416–20, 3 2007.

[3] S. Collins, A. Ruina, R. Tedrake, and M. Wisse, "Efficient bipedal robots based on passive-dynamic walkers," *Science*, vol. 307, no. 5712, pp. 1082–1085, 2005.

[4] A. D. Ames, "Human-inspired control of bipedal walking robots," *IEEE Transactions on Automatic Control*, vol. 59, no. 5, pp. 1115–1130, 5 2014.

[5] C. Della Santina, R. K. Katzschmann, A. Biechi, and D. Rus, "Dynamic control of soft robots interacting with the environment," in *2018 IEEE International Conference on Soft Robotics (RoboSoft)*. IEEE, 4 2018, pp. 46–53.

[6] F. Angelini, C. Della Santina, M. Garabini, M. Bianchi, and A. Bicchi, "Control architecture for human-like motion with applications to articulated soft robots," *Frontiers in Robotics and AI*, vol. 7, no. September, pp. 1–17, 2020.

[7] N. Correll, K. E. Bekris, D. Berenson, O. Brock, A. Causo, K. Hauser, K. Okada, A. Rodriguez, J. M. Romano, and P. R. Wurman, "Analysis and observations from the first amazon picking challenge," *IEEE Transactions on Automation Science and Engineering*, vol. 15, no. 1, pp. 172–188, 1 2018.

[8] F. F. Khalil and P. Payeur, "Dexterous robotic manipulation of deformable objects with multi-sensory feedback - a review," in *Robot Manipulators Trends and Development*. InTech, 3 2010, no. March 2010.

[9] D. McConachie, M. Ruan, and D. Berenson, "Interleaving planning and control for deformable object manipulation." Springer International Publishing, 2020, pp. 1019–1036.

[10] J. B. Dingwell, C. D. Mah, and F. A. Mussa-Ivaldi, "Experimentally confirmed mathematical model for human control of a non-rigid object," *Journal of Neurophysiology*, vol. 91, no. 3, pp. 1158–1170, 2004.

[11] M. Svinin, I. Goncharenko, V. Kryssanov, and E. Magid, "Motion planning strategies in human control of non-rigid objects with internal degrees of freedom," *Human Movement Science*, vol. 63, no. December 2018, pp. 209–230, 2019.

[12] A. J. Nagengast, D. A. Braun, and D. M. Wolpert, "Optimal control predicts human performance on objects with internal degrees of freedom," *PLoS Computational Biology*, vol. 5, no. 6, 2009.

[13] C. J. Hasson, T. Shen, and D. Sternad, "Energy margins in dynamic object manipulation," *Journal of Neurophysiology*, vol. 108, no. 5, pp. 1349–1365, 2012.

[14] M. C. Nah, A. Krotov, M. Russo, D. Sternad, and N. Hogan, "Dynamic primitives facilitate manipulating a whip," in *2020 8th IEEE RAS/EMBS International Conference for Biomedical Robotics and Biomechatronics (BioRob)*. IEEE, 11 2020, pp. 685–691.

[15] A. Krotov, "Human control of a flexible object: hitting a target with a bull-whip," Master's thesis, Northeastern University, 2020.

[16] B. Nasseroleslami, C. J. Hasson, and D. Sternad, "Rhythmic manipulation of objects with complex dynamics: predictability over chaos," *PLoS Computational Biology*, vol. 10, no. 10, 2014.

[17] S. Bazzi, J. Ebert, N. Hogan, and D. Sternad, "Stability and predictability in human control of complex objects," *Chaos*, vol. 28, no. 10, 2018.

[18] S. Bazzi and D. Sternad, "Robustness in human manipulation of dynamically complex objects through control contraction metrics," *IEEE Robotics and Automation Letters*, vol. 5, no. 2, pp. 2578–2585, 4 2020.

[19] R. Nayeem, S. Bazzi, N. Hogan, and D. Sternad, "Transient behavior and predictability in manipulating complex objects," pp. 10 155–10 161, 2020.

[20] H. Guang, S. Bazzi, D. Sternad, and N. Hogan, "Dynamic primitives in human manipulation of non-rigid objects," *Proceedings - IEEE International Conference on Robotics and Automation*, vol. 2019-May, pp. 3783–3789, 2019.

[21] P. Morasso, "Spatial control of arm movements," *Experimental Brain Research*, vol. 42, no. 2, pp. 223–227, 4 1981.

[22] T. Flash and N. Hogan, "The coordination of arm movements: an experimentally confirmed mathematical model," *The Journal of Neuroscience*, vol. 5, no. 7, pp. 1688–1703, 7 1985.

[23] T. Flash and E. Henis, "Arm trajectory modifications during reaching towards visual targets," *Journal of Cognitive Neuroscience*, vol. 3, no. 3, pp. 220–230, 1991.

[24] E. Todorov and M. I. Jordan, "Optimal feedback control as a theory of motor coordination," *Nature Neuroscience*, vol. 5, no. 11, pp. 1226–1235, 11 2002.

[25] E. Todorov, "Stochastic optimal control and estimation methods adapted to the noise characteristics of the sensorimotor system," *Neural Computation*, vol. 17, no. 5, pp. 1084–1108, 5 2005.

[26] J. Izawa, T. Rane, O. Donchin, and R. Shadmehr, "Motor adaptation as a process of reoptimization," *Journal of Neuroscience*, vol. 28, no. 11, pp. 2883–2891, 3 2008.

[27] D. Liu and E. Todorov, "Evidence for the flexible sensorimotor strategies predicted by optimal feedback control," *Journal of Neuroscience*, vol. 27, no. 35, pp. 9354–9368, 2007.

[28] S.-H. Yeo, D. W. Franklin, and D. M. Wolpert, "When optimal feedback control is not enough: feedforward strategies are required for optimal control with active sensing," *PLOS Computational Biology*, vol. 12, no. 12, p. e1005190, 12 2016.

[29] C. M. Harris and D. M. Wolpert, "Signal-dependent noise determines motor planning," *Nature*, vol. 394, no. 6695, pp. 780–784, 8 1998.

[30] J. Diedrichsen, R. Shadmehr, and R. B. Ivry, "The coordination of movement: optimal feedback control and beyond," *Trends in Cognitive Sciences*, vol. 14, no. 1, pp. 31–39, 1 2010.

[31] D. Sternad, W. J. Dean, and S. Schaal, "Interaction of rhythmic and discrete pattern generators in single-joint movements," *Human Movement Science*, vol. 19, no. 4, pp. 627–664, 10 2000.

[32] S. Schaal, S. Kotosaka, and D. Sternad, "Nonlinear dynamical systems as movement primitives," *International Conference on Humanoid Robotics Cambridge MA*, vol. 38, no. 2, p. 117–124, 2001.

[33] S. Schaal, "Is imitation learning the route to humanoid robots?" *Trends in Cognitive Sciences*, vol. 3, no. 6, pp. 233–242, 6 1999.

[34] A. J. Ijspeert, J. Nakanishi, H. Hoffmann, P. Pastor, and S. Schaal, "Dynamical movement primitives: learning attractor models for motor behaviors," *Neural Computation*, vol. 25, no. 2, pp. 328–373, 2 2013.

[35] A. Ijspeert, J. Nakanishi, and S. Schaal, "Movement imitation with nonlinear dynamical systems in humanoid robots," in *Proceedings 2002 IEEE International Conference on Robotics and Automation (Cat. No.02CH37292)*, vol. 2, no. May. IEEE, 2002, pp. 1398–1403.

[36] P. Pastor, L. Righetti, M. Kalakrishnan, and S. Schaal, "Online movement adaptation based on previous sensor experiences," in *2011 IEEE/RSJ International Conference on Intelligent Robots and Systems*. IEEE, 9 2011, pp. 365–371.

[37] A. Ude, A. Gams, T. Asfour, and J. Morimoto, "Task-specific generalization of discrete and periodic dynamic movement primitives," *IEEE Transactions on Robotics*, vol. 26, no. 5, pp. 800–815, 10 2010.

[38] R. Ronsse, D. Sternad, and P. Lefèvre, "A computational model for rhythmic and discrete movements in uniand bimanual coordination," *Neural Computation*, vol. 21, no. 5, pp. 1335–1370, 2009.

[39] A. De Rugy and D. Sternad, "Interaction between discrete and rhythmic movements: Reaction time and phase of discrete movement initiation during oscillatory movements," *Brain Research*, vol. 994, no. 2, pp. 160–174, 2003.

[40] N. Hogan and D. Sternad, "Dynamic primitives of motor behavior," *Biological Cybernetics*, vol. 106, no. 11-12, pp. 727–739, 2012.

[41] S. H. Scott, "Optimal feedback control and the neural basis of volitional motor control," *Nature Reviews Neuroscience*, vol. 5, no. 7, pp. 532–544, 2004.

[42] F. Crevecoeur, S. H. Scott, and T. Cluff, "Robust control in human reaching movements: a model-free strategy to compensate for unpredictable disturbances," *The Journal of neuroscience : the official journal of the Society for Neuroscience*, vol. 39, no. 41, pp. 8135–8148, 2019.

[43] A. Billard, S. Calinon, R. Dillmann, and S. Schaal, "Robot programming by demonstration," in *Springer Handbook of Robotics*. Berlin, Heidelberg: Springer Berlin Heidelberg, 2008, vol. 6, no. 9-10, pp. 1371–1394.

[44] S. Schaal, A. Ijspeert, and A. Billard, "Computational approaches to motor learning by imitation," *Philosophical Transactions of the Royal Society of London. Series B: Biological Sciences*, vol. 358, no. 1431, pp. 537–547, 3 2003.

[45] E. Gribovskaya, A. Kheddar, and A. Billard, "Motion learning and adaptive impedance for robot control during physical interaction with humans," in *2011 IEEE International Conference on Robotics and Automation*. IEEE, 5 2011, pp. 4326–4332.

[46] J. Hermus, J. Doeringer, D. Sternad, and N. Hogan, "Separating neural influences from peripheral mechanics: The speed-curvature relation in mechanically constrained actions," *Journal of Neurophysiology*, vol. 123, no. 5, pp. 1870–1885, 2020.

[47] N. Hogan and D. Sternad, "Dynamic primitives in the control of locomotion," *Frontiers in Computational Neuroscience*, vol. 7, no. MAY, pp. 1–16, 2013.

[48] M. Dimitriou, D. M. Wolpert, and D. W. Franklin, "The temporal evolution of feedback gains rapidly update to task demands," *Journal of Neuroscience*, vol. 33, no. 26, pp. 10 898–10 909, 2013.

[49] S. Bazzi and D. Sternad, "Human control of complex objects: towards more dexterous robots," *Advanced Robotics*, vol. 34, no. 17, pp. 1137–1155, 2020.

[50] P. Maurice, N. Hogan, and D. Sternad, "Predictability, force, and (anti)resonance in complex object control," *Journal of Neurophysiology*, vol. 120, no. 2, pp. 765–780, 8 2018.

[51] E. Burdet, R. Osu, D. W. Franklin, T. E. Milner, and M. Kawato, "The central nervous system stabilizes unstable dynamics by learning optimal impedance," *Nature*, vol. 414, no. 6862, pp. 446–449, 2001.

[52] D. Rancourt and N. Hogan, "Stability in force-production tasks," *Journal of Motor Behavior*, vol. 33, no. 2, pp. 193–204, 2001.

[53] B. Berret and F. Jean, "Stochastic optimal open-loop control as a theory of force and impedance planning via muscle co-contraction," *PLOS Computational Biology*, vol. 16, no. 2, p. e1007414, 2 2020.

[54] M. S. Shourijeh and B. J. Fregly, "Muscle synergies modify optimization estimates of joint stiffness during walking," *Journal of Biomechanical Engineering*, vol. 142, no. 1, pp. 1–9, 1 2020.

[55] H. Ravichandar, A. S. Polydoros, S. Chernova, and A. Billard, "Recent advances in robot learning from demonstration," *Annual Review of Control, Robotics, and Autonomous Systems*, vol. 3, no. 1, pp. 297–330, 5 2020.